



Fermi National Accelerator Laboratory

FERMILAB-Conf-97/343-E

D0

Preliminary Results from the D-Zero Silicon Vertex Beam Tests

Maria Teresa P. Roco
For the D0 Collaboration

*Fermi National Accelerator Laboratory
P.O. Box 500, Batavia, Illinois 60510*

October 1997

Submitted to *Nuclear Instruments and Methods A* and Published Proceedings of the *6th International Workshop on Vertex Detectors (VERTEX'97)*, Mangaratiba, Rio de Janeiro, Brazil,
August 31-September 5, 1997

Disclaimer

This report was prepared as an account of work sponsored by an agency of the United States Government. Neither the United States Government nor any agency thereof, nor any of their employees, makes any warranty, expressed or implied, or assumes any legal liability or responsibility for the accuracy, completeness, or usefulness of any information, apparatus, product, or process disclosed, or represents that its use would not infringe privately owned rights. Reference herein to any specific commercial product, process, or service by trade name, trademark, manufacturer, or otherwise, does not necessarily constitute or imply its endorsement, recommendation, or favoring by the United States Government or any agency thereof. The views and opinions of authors expressed herein do not necessarily state or reflect those of the United States Government or any agency thereof.

Distribution

Approved for public release; further dissemination unlimited.

Preliminary Results from the D-Zero Silicon Vertex Beam Tests ¹

Maria Teresa P. Roco ²
for the D-Zero Collaboration

*Fermi National Accelerator Laboratory
Batavia, IL. 60510 USA*

Abstract

Extensive tests of the D-Zero silicon vertex detectors and the final version of the SVX-II chip and readout electronics were performed at a test beam facility equipped with a 2 Tesla magnet at FNAL. Preliminary results are reported on the performance of the SVX-II chip, charge collection properties, signal to noise ratio, cluster pulse height and spatial resolution.

1 Introduction

Run II of the Fermilab Tevatron collider is scheduled to begin in 1999. With the proposed accelerator parameters we expect over a tenfold increase in the luminosity up to $2 \times 10^{32} /cm^2/s$. In addition, the bunch crossing interval will decrease from $3.5 \mu s$ to $132 ns$. The $D0$ detector is currently being upgraded in order to optimize its physics reach in Run II. An integral part of the $D0$ upgrade [1], the silicon vertex detector [2] will be a critical component in the identification of $t\bar{t}$ events. Directly surrounding the beam interaction region, the silicon tracker has the capability to discriminate tracks originating from decays of long-lived particles and to precisely determine the primary interaction vertex. The design specifications for the silicon detectors were chosen to give good spatial resolution, minimum noise in the readout electronics and maximum radiation tolerance.

¹ Presented at the 6th International Workshop on Vertex Detectors (VERTEX '97), Aug. 31- Sept. 5, 1997, Mangaratiba, Rio de Janeiro

² Email: *roco@fnal.gov*

Recently, we have performed extensive tests of the silicon detectors at a test beam at Fermilab. Several single-sided silicon detectors and a prototype small angle double-sided detector were tested with the final version of the SVX-II chip and the readout electronics. The readout frequency was set at 53 MHz. Preliminary results on the performance of the SVX-II chip, charge collection properties, signal to noise ratio, cluster pulse height and spatial resolution are presented for the single-sided test ladders. Studies on radiation damage effects based on tests performed on a previously irradiated detector are also shown.

2 Test devices and test beam setup

The test devices included four beam telescope elements using six single-sided $50\ \mu\text{m}$ pitch silicon detectors operating at $35\ \text{V}$ bias voltage. They are fabricated on n -type silicon of $300\ \mu\text{m}$ thickness. Each detector has 384 strips read out by three 128-channel SVX-II chips. The detectors are AC-coupled to the readout electronics by capacitors integrated directly onto each strip. The coupling capacitor is formed by a $200\ \text{nm}$ dielectric (SiO_2) layer between the strip implant and the Al metalization. Polysilicon resistors ($2\ \text{M}\Omega$) are used to bias the strips.

Beam tests were performed at Fermilab N-West with a $125\ \text{GeV}$ charged pion beam. The test beam setup is shown schematically in Fig. 1. Four detectors were used as vertical sensors (v) and two were used as horizontal sensors (h) providing six space points in x and y to measure the trajectory of the incoming beam particle. The coincidence of four scintillator counters located upstream and downstream of the telescope elements provided the beam trigger. To simulate the superconducting solenoid in the upgraded detector, the test beam setup included a magnet which can provide a \vec{B} field of up to 2 Tesla. The magnetic field is in the direction parallel to the detector strips.

A test ladder, constructed by wire-bonding two detectors together, is mounted on a remotely controlled movable table allowing rotation around the vertical axis as well as translation in the horizontal and vertical directions perpendicular to the beam. Rotations around the horizontal axis are done manually. The reference frame is shown in Fig. 2 with the z -axis along the beam direction. The x -axis is parallel to detector strips.

Two single-sided test ladders were tested including one previously irradiated up to 1 MRad. For angular dependence studies data were taken with the plane of the test detector rotated at several values of θ and ϕ . A partially instrumented prototype double-sided 2° detector was also tested. Results for the double-sided detector will be presented in a later publication.

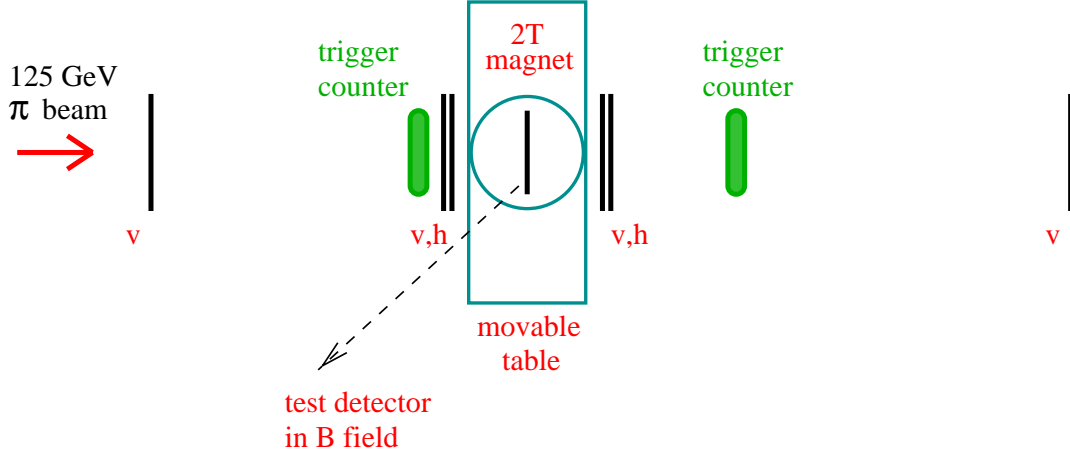


Fig. 1. Test beam setup. Shown are four telescope elements and a remotely controlled movable table where test detectors are mounted.

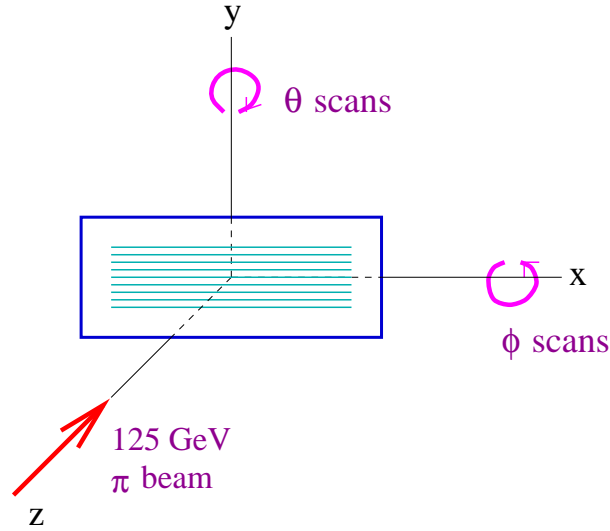


Fig. 2. The z -axis is parallel to the beam direction, while the x -axis is parallel to the detector strips. Data were taken with the plane of the test detector rotated for several values of θ and ϕ . The magnetic field is in the direction parallel to the detector strips and can be varied up to 2 Tesla.

2.1 Readout System

The charge on each silicon strip, stored as a voltage across a capacitor, is digitized by the SVX-II chip which is wire-bonded directly to the detector. The SVX-II chips are connected to a kapton/copper flexible printed circuit, the High Density Interconnect (HDI), containing an 8-bit data bus, clock and control line traces, bypass capacitors, resistors for chip biasing, and a “tail” for external connections. Port cards control the operation of the SVX-II chips by sending clock pulses and control signals across an 8.5 m cable connected to the HDI. The SVX-II chips respond by sending channel and data information

back to the port cards. Data is sent to the VME Readout Buffer(VRB) module via an optical link. A controller card in the VME crate acts as the interface between the VRB module and the rest of the data acquisition system.

A more detailed description of the silicon vertex detector, the SVX-II chip and the readout electronics are given in [2] and in this proceedings [3].

3 Single-sided Test Ladder Results

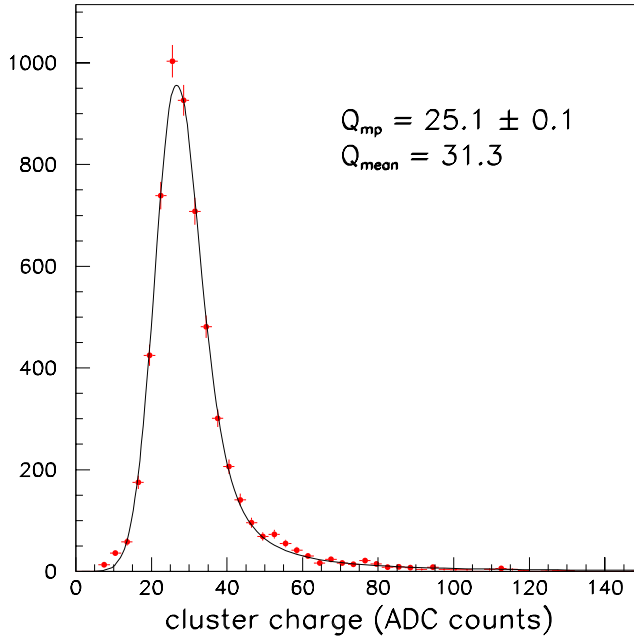


Fig. 3. Test ladder cluster charge distribution for 125 GeV charged pions at normal incidence with $B = 2$ Tesla. A most probable value of 25 ADC counts is obtained by fitting a Gaussian convoluted Landau distribution. This corresponds to a signal to noise ratio of about 18.

For each event the coherent baseline shift is obtained by fitting the raw pulse heights distribution of all 128 channels of an SVX chip with a Gaussian. The raw pulse height of every channel is corrected for this baseline shift to obtain the pedestal. The average random noise level is the Gaussian width of the pedestal distribution. The values of σ_N^i of the same SVX chip are uniform with an average channel to channel variation typically less than 1 ADC count.

A selection criteria was applied in order to separate signals from noise. The baseline corrected pulse heights of each channel are scanned for signals larger than five times the random noise σ_N of the channel. A cluster charge is defined

as the sum of this signal and the signals of all contiguous channels i above $2\sigma_N^i$. The cluster position is defined as the charge centroid, $x_o = \frac{\sum_i Q_i x_i}{\sum_i Q_i}$, where the sum is over all the constituent strips. Clusters which include bad channels are excluded. Fig. 3 shows the cluster charge distribution of the single-sided test ladder for 125 GeV charged pions at normal incidence with $B = 2$ Tesla.

The signal to noise ratio S/N is defined as Q_{mp}/σ_N , where Q_{mp} is the most probable value of the cluster charge. To determine Q_{mp} the cluster charge in Fig. 3 is fitted with a Gaussian convoluted Landau distribution as shown. Since the channel to channel variation of σ_N^i for the same SVX-II chip is small, the average is used in this analysis. A signal to noise ratio of about 18 was obtained for the single-sided test ladder.

Data were taken at various θ and ϕ incidence angles and at various magnetic field settings. For $B = 0$ (circles) and $B = 2$ Tesla (squares), the most probable value of the cluster charge is plotted as a function of θ in Fig. 4, in good agreement with the geometric scaling of Q with $1/\cos\theta$ shown as the dashed curve. The charge pulse height and the width of the pulse height distribution are independent of the magnetic field.

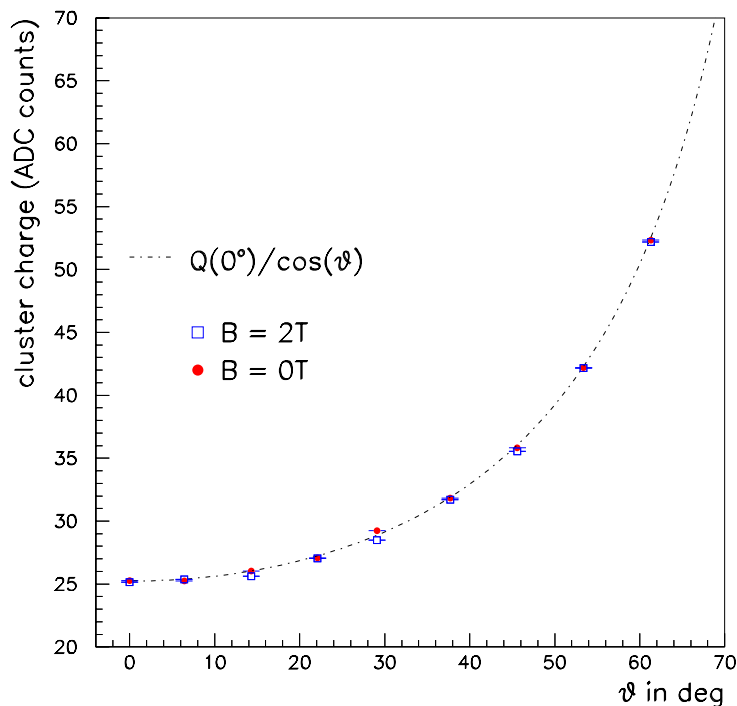


Fig. 4. The cluster charge Q_{mp} is plotted as a function of the incidence angle θ for $B = 0$ Tesla (circles) and 2 Tesla (squares) in good agreement with the geometric scaling of Q with $1/\cos\theta$.

The spatial resolution was studied by performing an unweighted linear least squares fit on the particle track using special alignment runs where the magnet was taken out of the beam line. There were three parameters used in the fit corresponding to the four telescope elements (v coordinates) and excluding the second element, TBT2. The residuals, shown in Fig. 5, represent the difference between the linear fit and the measured position in TBT2. These residuals contain the contributions from the intrinsic resolution and the systematic uncertainty from multiple Coulomb scattering. Correcting for these contributions, we obtain a spatial resolution consistent with $10\text{ }\mu\text{m}$.

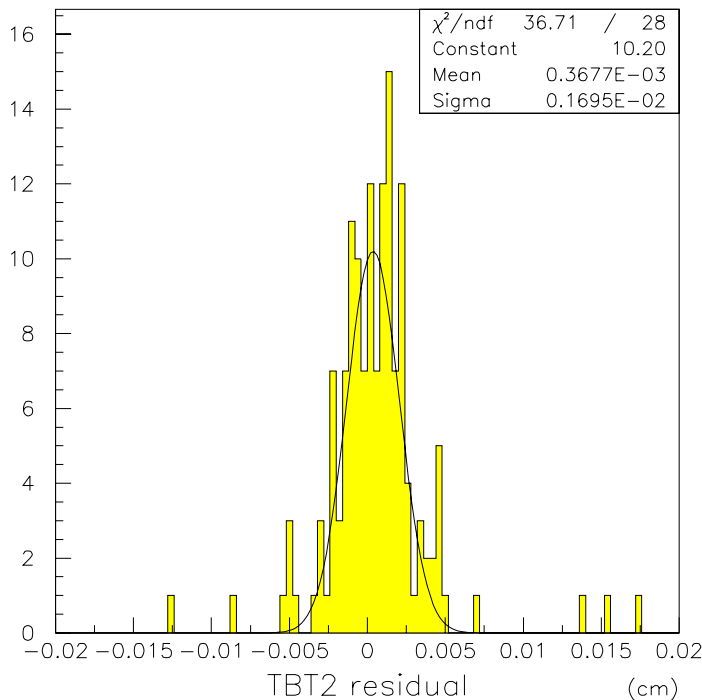


Fig. 5. The residuals representing the difference between the linear fit and the measured position in telescope element TBT2. These residuals contain the intrinsic resolution and the systematic uncertainty from multiple Coulomb scattering.

4 Irradiated Test Ladder Results

We have also tested a single-sided ladder which was previously irradiated up to $1\text{ MRad} \pm 15\%$ with 8 GeV protons at the Fermilab booster facility. This ladder was stored in room temperature for 4 months after irradiation. The ladder operated at a bias voltage of 120 V based on laser test stand measurements. Fig.6 shows the depletion voltage curve as a function of bias voltage, where the

y-axis is the number of counts normalized to unity. The irradiated ladder shows a much slower rise compared to the non-irradiated ladder. These measurements also show that the irradiated ladder was functional at greater than 200 V bias voltage and did not show any sign of breakdown.

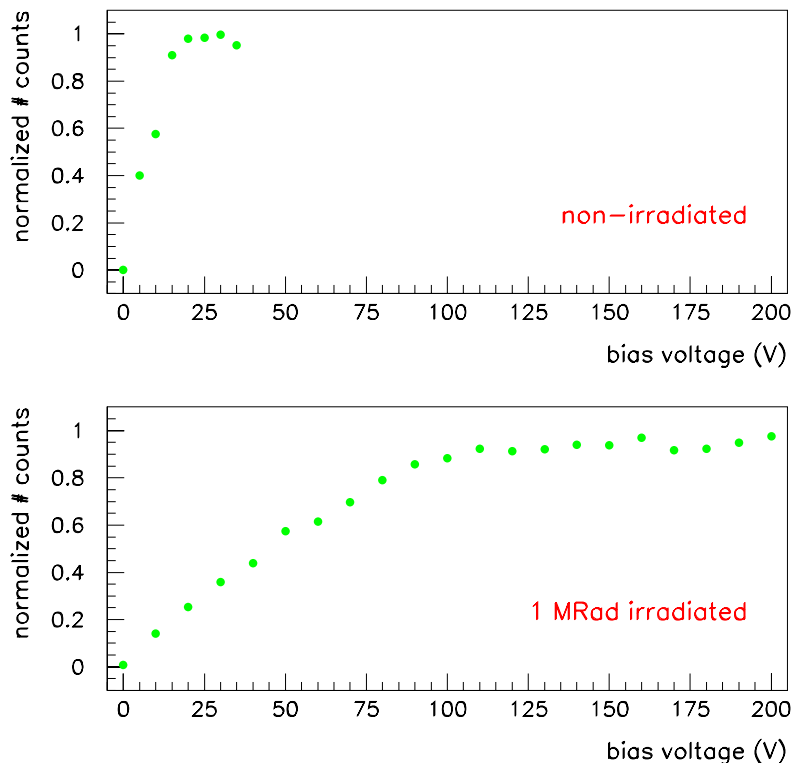


Fig. 6. Depletion voltage measurements from the laser test stand. The vertical axis is in arbitrary units normalized to one. The irradiated ladder shows a much slower rise compared to the non-irradiated ladder.

From the test beam data for normally incident 125 GeV charged pions, the cluster charge Q_{mp} with $B = 2$ Tesla was measured to be 30 % lower compared to the single-sided non-irradiated ladder. We also studied the dependence of the cluster charge and noise on the chip parameters such as the ramp trim and preamplifier band width (PABW) [‡]. Radiation damage effects include an increase in the detector leakage current and a corresponding increase in noise. We observed this increase by comparing the random noise, expressed in number of electrons referred to as the equivalent noise charge, plotted as a function of the PABW in Fig. 7 for both the irradiated and non-irradiated

[‡] For different bunch crossing or interaction times, the response or the bandwidth of the SVX-II preamplifier is adjusted by means of internal switches and capacitors to provide the optimal preamplifier output risetime and hence minimum noise.

single-sided test ladders. The irradiated ladder was operated at room temperature with a leakage current of $1 \mu A/\text{strip}$. The measured noise is consistent with being dominated by shot noise due to leakage current.

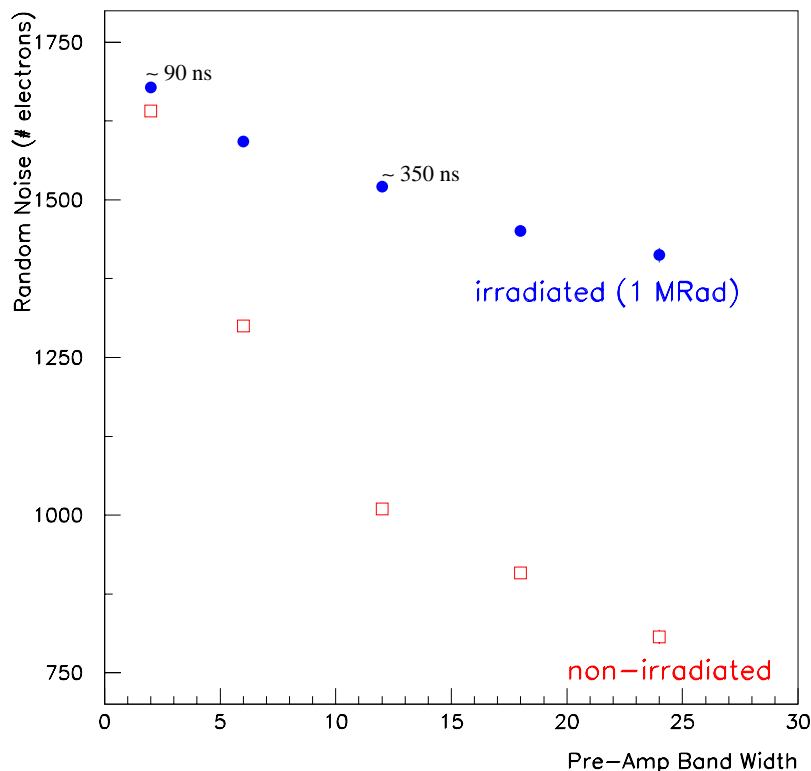


Fig. 7. The random noise expressed in number of electrons, referred to as the equivalent noise charge, is plotted as a function of the preamplifier bandwidth for both the irradiated and non-irradiated single-sided test ladders.

5 Summary

We have performed extensive tests of the *D0* silicon vertex system, with the final version of the SVX-II chip and the readout electronics, at a Fermilab test beam facility equipped with a 2 Tesla magnet. Under test beam conditions the system proved to work quite well. The study of the angular dependence of the cluster charge shows good agreement with the expected geometrical scaling with $1/\cos\theta$. With a signal to noise ratio of 18 for the single-sided test ladders, the spatial resolution for perpendicular tracks is determined to be consistent with $10 \mu m$ using an unweighted linear fit. Studies on radiation

damage effects based on tests performed with a detector previously irradiated up to 1 MRad show a substantial increase in the depletion voltage and equivalent noise charge. Comparison with a non-irradiated ladder show that the cluster charge in the irradiated detector is degraded by as much as 30 %. From laser test stand measurements, we did not observe the breakdown of the irradiated detector for voltages up to 200 V indicating that the breakdown voltage was well above depletion voltage. These studies give us confidence that the silicon vertex detector will function until the end of Run II.

References

- [1] *D0 Upgrade Technical Design Report*
- [2] *D0 Silicon Tracker Technical Design Report*, *D0-Note 2169* (unpublished)
- [3] see Ron Lipton's talk